Compact fiber-optic curvature sensor based on super-mode interference in a seven-core fiber

G. Salceda-Delgado,[1,2,*] A. Van Newkirk,[1] J. E. Antonio-Lopez,[1] A. Martinez-Rios,[2] A. Schülzgen,[1] and R. Amezcua Correa[1]

[1]CREOL, The College of Optics & Photonics, University of Central Florida, P.O. Box 162700, Orlando, Florida 32816-2700, USA

[2]Centro de Investigaciones en Optica A. C., Loma del Bosque 115, León Gto. 37150, Mexico

*Corresponding author: Guillermo.salceda@ucf.edu

Received December 19, 2014; revised February 20, 2015; accepted February 25, 2015; posted February 27, 2015 (Doc. ID 231103); published March 27, 2015

A compact, low loss, and highly sensitive optical fiber curvature sensor is presented. The device consists of a few-millimeter-long piece of seven-core fiber spliced between two single-mode fibers. When the optical fiber device is kept straight, a pronounced interference pattern appears in the transmission spectrum. However, when the device is bent, a spectral shift of the interference pattern is produced, and the visibility of the interference notches changes. This allows for using either visibility or spectral shift for sensor interrogation. The dynamic range of the device can be tailored through the proper selection of the length of the seven-core fiber. The effects of temperature and refractive index of the external medium on the response of the curvature sensor are also discussed. Linear sensitivity of about 3000 nm/mm^{-1} for bending was observed experimentally.

OCIS codes: (060.2280) Fiber design and fabrication; (060.2370) Fiber optics sensors.

http://dx.doi.org/10.1364/OL.40.001468

The measurement of mechanical deformation, related to the mechanical parameter curvature radius, is of importance in structural monitoring applications. Optical fiber sensors are well suited for this application due to their unique advantages over traditional sensors, such as their light weight, compactness, stability, fast response, high sensitivity, repeatability, insensitivity to electromagnetic interference, and so on. To date, there are many kinds of optical fiber sensors with varying responses to perturbation from external parameters. For measurements of external physical parameters, one of the most attractive optical fiber sensor configurations is based on the Mach–Zehnder interferometer [1–7]. Specialty optical fibers, such as photonic crystal fiber and multicore fiber (MCF), have also been used for sensing applications [1,7–10]. These specialty optical fibers have shown good performance, simplicity, and great sensitivity to various external parameters due to their unique characteristics.

Here, we utilize the light propagation in a MCF, where so-called super-modes are supported by the fiber structure [11], to design and fabricate a seven-core fiber to be implemented as a bending sensor. Keeping the distance between cores of the MCF small, energy can be transferred between different cores, allowing super-modes to propagate down the length of the MCF and to interfere during propagation. This super-mode interference is very sensitive to external mechanical disturbances such as bending. We will demonstrate that it is possible to take advantage of this sensitivity and to construct a robust and attractive seven-core optical fiber bending sensor.

The structure of the seven-core fiber sensor is very simple. It consists of a few millimeters of sensing fiber (seven-core fiber) spliced between two single-mode fibers (SMF). Using this MCF configuration, no further fabrication steps where specialized equipment could be required are necessary. This is a great advantage, especially compared to those approaches that require complex glass-processing machines to fabricate sensing structures. Similar structures, with a sensing fiber spliced between two single-mode fibers, have been used in previous works [1,7,8,12–17] showing that this approach is indeed suitable for various sensing applications, while exhibiting simplicity and easy manufacturing. The fabrication of the device only requires the use of a standard fusion splicing machine. Typical insertion losses through the complete device are around 0.026 dB. These negligible losses allow several devices to be spliced in line in order to make a multi-point bending sensor.

The MCF used in the curvature sensor is composed of seven strongly coupled germanium-doped cores. Each core has a diameter of 9.2 μm and a NA of 0.132. The core-to-core separation is 11 μm, and the cladding diameter is 125 μm, similar to the seven-core fiber used in previous experiments [18,19]. The MCF supports seven super-modes; however, as a result of the excitation by the fundamental mode of a SMF, only the two super-modes with nonzero intensity in the central core have modal overlap and are, therefore, excited [18]. After propagation through the seven-core fiber segment, the excited super-modes are re-coupled into the second SMF, and a periodic transmission spectrum is generated as a result of the interference between them. As the fiber is bent, the refractive index profile becomes asymmetric due to elasto-optic and geometrical changes in the refractive index. This generates a differential phase delay between the propagating super-modes that depends on the curvature radius. Hence, the bending radius can be found by monitoring the wavelength shift and visibility of the interference notches in the transmission spectrum.

The structure of the sensor, the setup used to characterize its response to bending, and the seven core fiber cross-section are shown in Fig. 1. The sensors were characterized in transmission using a superluminiscent diode (Thorlabs SLD1550S-A1) as the light source, and the detection was carried out with an optical spectrum analyzer (OSA) (Agilent model 86146B). Each sensor device was placed and secured in a v-groove made on a thin sheet of metal of 316 mm in length, whose ends were fixed to translation stages so that by a relative inward movement of the translation stages the curvature radius could be

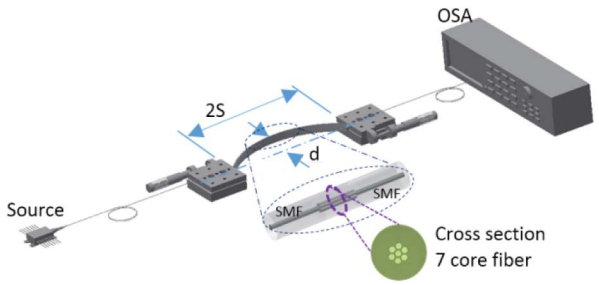

Fig. 1. Setup used to characterize the bending response of the MCF sensor [2]. Inset is the structure of the sensor and the cross-section picture of the seven-core fiber that is spliced between two SMF.

varied. The dimensions S and d indicated in Fig. 1, were used to calculate the bending radius R, using the well-known relation $1/R = 2d/(d^2 + S^2)$ [20].

The transmission spectra of sensor devices with seven core fiber lengths of 18 mm and 10 mm, respectively, are shown in Fig. 2 for three different inverse curvature radii. Note that both the peak wavelengths and the amplitude of the modulation are dependent on the radius of curvature of the fiber, while the fringe period remains almost constant. The relationship between fringe separation and inverse length of seven-core fiber is shown in Fig. 3, which shows that the fringe period is linearly dependent on the inverse of the length of seven-core fiber segment with a factor of 1294 nm/mm^{-1}.

In interferometric applications, fringe visibility is used to evaluate the quality of the fringe pattern [2]. Here we found that both the visibility and the wavelength shift of the fringes were strongly dependent on the bending radius of the MCF devices. The observed change in fringe visibility is a consequence of the field becoming radiative as the MCF is bent to certain curvature radii [21].

The well-known relationship

$$V = \frac{I_{\text{upp,min}} - I_{\text{low,min}}}{I_{\text{upp,min}} + I_{\text{low,min}}} \tag{1}$$

was used to calculate the visibility [22]. Where $I_{\text{upp,min}}$ and $I_{\text{low,min}}$ are the minimums of the upper and lower

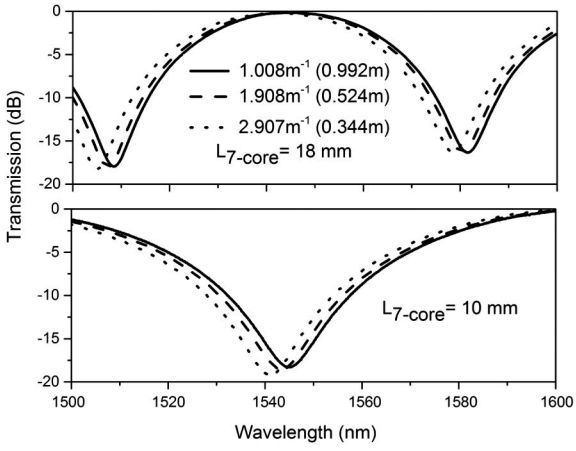

Fig. 2. Sensor device spectra when the length of the seven-core fiber segment is 18 mm (upper graph) and 10 mm (bottom graph) for three different bending radii.

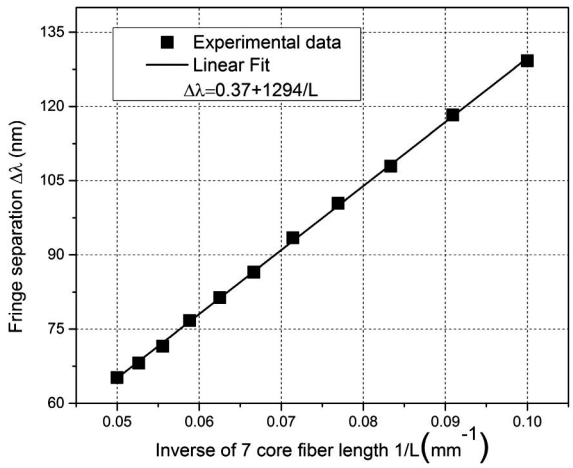

Fig. 3. Measured relationship between inverse length of seven-core fiber segment, 1/L, and interference fringe separation, $\Delta\lambda$, of the fabricated sensor devices (linear dependence).

envelopes of the transmission spectra, respectively. The measured fringe visibility versus inverse curvature radius for the lengths 10, 16, and 25 mm of seven-core fibers is shown in Fig. 4. From a linear fit we obtained the slopes of 3.47 a.u./mm^{-1}, 2.39 a.u./mm^{-1}, and 3.86 a.u./mm^{-1}, respectively.

With the devices kept straight, the transmission spectra have initial visibility values. This initial value can be considered as the zero bending condition. As the sensor device is bent, or more accurately, when the inverse bending radius increases, the visibility grows approximately linear. Taking into consideration that the limiting and maximum value of the visibility is unity, it is inferred that longer length devices can be used to measure larger inverse radii, whereas shorter lengths can be used to measure smaller inverse radii (see Fig. 4).

In addition to this method of interrogation via visibility, the bending can be alternatively measured by the wavelength shift of the spectral interference features. The dependence of the transmission notch wavelength on the inverse bending radius for the sensor device with 10 mm of seven core fiber is shown in Fig. 5. The most

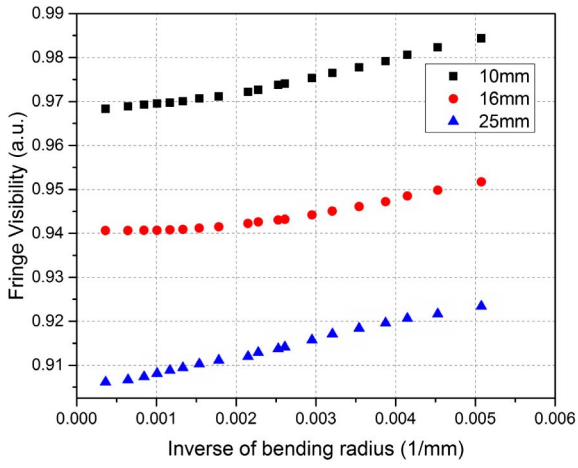

Fig. 4. Fringe visibility versus inverse curvature radius for three different seven-core fiber lengths: 10 mm (squares), 16 mm (circles), and 25 mm (triangles).

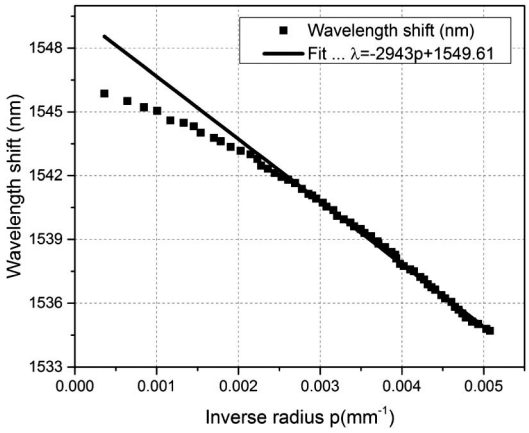

Fig. 5. Transmission notch wavelength versus inverse bending radius of the sensor device length with 10 mm of seven-core fiber. Linear fit of the most sensitive area is shown in the range of 0.0022–0.005 mm^{-1} or 200 to 450 mm speaking in terms of bending radius.

sensitive bending radius region is between 0.0022 mm^{-1} (450 mm) and 0.005 mm^{-1} (200 mm). Here, the sensitivity is −2943 nm/mm^{-1}, as seen in Fig. 5. However, for inverse radius values below 0.002 mm^{-1}, the sensitivity drops to −1653.7 nm/mm^{-1}. Sensor devices with different lengths have been tested, and a similar wavelength shift behavior to that shown in Fig. 5 was observed.

Similar but slightly different changes in both fringe visibility and wavelength shift were observed when the device was bent in the opposite direction. Figure 6 illustrates the spectral response of a 5-mm-long MCF device. The continuous curve represents the MCF sensor bent in one direction, and the dashed curve shows the sensor bent in the opposite direction at 0.00178, 0.00269, and 0.00337 mm^{-1} of inverse curvature radii. These differences could be due to small variations in the symmetry changes of the seven-core fiber as it is bent, since it is difficult to ensure that the outer core fiber orientation is exactly the same when the bending direction is changed. This might lead to slightly different

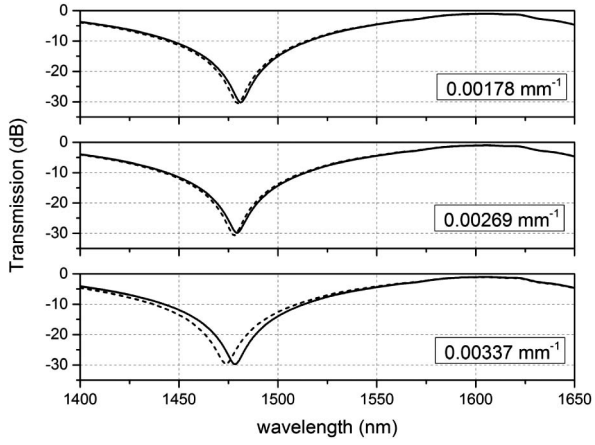

Fig. 6. Spectral response of a device with 5 mm of MCF length that has been bent in two opposite directions. The continuous curve is one direction, and the dash curve represents the opposite direction at three different inverse curvature radii (0.00178 mm^{-1}, 0.00269 mm^{-1}, and 0.00337 mm^{-1}).

conditions with regard to the effective elasto-optic coefficient of the fiber when bent in opposite directions. However, such effects could possibly be exploited to identify the direction of the observed bending.

Most fiber sensors are embedded into a solid protection matrix, and sometimes the behavior of the sensor may change because of the RI of the matrix. However, in our case, the seven-core fiber sensors are not sensitive to external refractive indices because the light is very well confined in the cores of the MCF. This is a clear advantage that cannot be found in many other fiber sensors, such as those based on the interaction with the evanescent part of the fiber modes.

The effect of temperature on the response of the sensor was also analyzed. We observed a wavelength peak shift of about 4 nm going from room temperature to 100 degrees Celsius, and a slight variation on the visibility while the sensor was kept straight. This effect can be discarded if in the bending measurement the temperature remains constant or is separated by using a bending insensitive temperature sensor.

In conclusion, a robust, very easy to construct, and highly bend-sensitive optical fiber sensor based on a specially designed seven-core fiber has been demonstrated. The seven-core fiber acts as the sensor head, spliced between two SMFs, forming a compact device with negligible insertion loss. It can be interrogated by either fringe visibility or wavelength peak shift. Its operating principle is based on the interference between two super-modes excited by the fundamental mode of the input SMF. The bending of the sensor induces a wavelength shift of interference features and changes in the amplitude of modulation (visibility). When it is interrogated by visibility, its dynamic range can be tailored by the proper selection of the length of the seven-core fiber segment. When it is interrogated by wavelength shift, it has a sensitivity of around 3000 nm/mm^{-1} in terms of inverse curvature in the range from 200 to 450 mm bending radius. It can be embedded in, or coated with, a protective material without affecting its performance due to its insensitivity to external RI. These characteristics of the sensor make it very attractive for structural monitoring applications.

G. Salceda-Delgado would like to thank Consejo Nacional de Ciencia y Tecnologia (CONACYT) for the scholarship granted to him. This work was supported by FAZ Technology Inc.

References

1. M. Deng, C. P. Tang, T. Zhu, and Y. J. Rao, Opt. Commun. **284**, 2849 (2011).
2. D. Monzon-Hernandez, A. Martinez-Rios, I. Torres Gomez, and G. Salceda-Delgado, Opt. Lett. **36**, 4380 (2011).
3. Q. Q. Meng, X. Y. Dong, Y. Zhou, K. Ni, Z. M. Chen, C. L. Zhao, and S. Z. Jin, J. Electron. Waves Appl. **26**, 2438 (2012).
4. R. Wang, J. Zhang, Y. Weng, Q. Rong, Y. Ma, Z. Feng, M. Hu, and X. Qiao, IEEE Sensors J. **13**, 1766 (2013).
5. Z. Tian, S. S.-H. Yam, and H. Loock, IEEE Photon. Technol. Lett. **20**, 1387 (2008).
6. O. Frazão, J. Viegas, P. Caldas, J. L. Santos, F. M. Araújo, L. A. Ferreira, and F. Farahi, Opt. Lett. **32**, 3074 (2007).
7. W. Chang Wong, C. Chiu Chan, H. Gong, and K. Chew Leong, IEEE Photon. Technol. Lett. **23**, 795 (2011).

8. R. M. Silvia, M. S. Ferreira, J. Kobelke, K. Schuster, and O. Frazão, Opt. Lett. **36**, 939 (2011).
9. H. P. Gong, C. C. Chan, P. Zu, L. H. Chen, and X. Y. Dong, Opt. Commun. **283**, 3142 (2010).
10. R. Jha, J. Villatoro, G. Badenes, and V. Pruneri, Opt. Lett. **34**, 617 (2009).
11. D. Dorosz and M. Kochanowicz, Opto-Electron. Rev. **19**, 40 (2011).
12. S. Silva, O. Frazão, J. Viegas, L. A. Ferreira, F. M. Araújo, F. X. Malcata, and J. L. Santos, Meas. Sci. Technol. **22**, 085201 (2011).
13. J. R. Guzman-Sepulveda, R. Dominguez-Cruz, J. J. Sánchez-Mondragón, and D. A. May-Arrioja, "Curvature sensor based on a two-core optical fiber," in *Quantum Electronics and Laser Science Conference (CLEO)*, OSA Technical Digest (Optical Society of America, 2012), paper JW2A.116.
14. G. Chunying and Y. Libo, "Supermodes Analysis for linearly distributed multicore fiber," in *The International Symposium on Photonics and Optoelectronics (SOPO)*, Wuhan, China, August 14–16, 2009, pp. 1–4.
15. J. Chen, J. Zhou, and Z. Jia, IEEE Photon. Technol. Lett. **25**, 2354 (2013).
16. Y. Liu, L. Zhang, J. A. R. Williams, and I. Bennion, IEEE Photon. Technol. Lett. **12**, 531 (2000).
17. L. Niu, C. Zhao, H. Gong, Y. Li, and S. Jin, Opt. Commun. **333**, 11 (2014).
18. A. Van Newkirk, E. Antonio-Lopez, G. Salceda-Delgado, R. Amezcua-Correa, and A. Schülzgen, Opt. Lett. **39**, 4812 (2014).
19. J. E. Antonio-Lopez, Z. Sanjabi Eznaveh, P. LikamWa, A. Schülzgen, and R. Amezcua-Correa, Opt. Lett. **39**, 4309 (2014).
20. W. Du, H. Tam, M. Liu, and X. Tao, Proc. SPIE **3330**, 284 (1998).
21. D. Marcuse, J. Opt. Soc. Am. **66**, 216 (1976).
22. E. H. Hecht, *Optics* (Addison-Wesley, 1987).